Journal of Materials Chemistry B

Accepted Manuscript

This is an *Accepted Manuscript*, which has been through the Royal Society of Chemistry peer review process and has been accepted for publication.

Accepted Manuscripts are published online shortly after acceptance, before technical editing, formatting and proof reading. Using this free service, authors can make their results available to the community, in citable form, before we publish the edited article. We will replace this *Accepted Manuscript* with the edited and formatted *Advance Article* as soon as it is available.

You can find more information about *Accepted Manuscripts* in the Information for Authors.

Please note that technical editing may introduce minor changes to the text and/or graphics, which may alter content. The journal's standard Terms & Conditions and the Ethical guidelines still apply. In no event shall the Royal Society of Chemistry be held responsible for any errors or omissions in this *Accepted Manuscript* or any consequences arising from the use of any information it contains.

ROYAL SOCIETY OF CHEMISTRY

www.rsc.org/materialsB

Solution Processed Carbon Nanotubes Modified Conducting Paper Sensor for Cancer Detection

Saurabh Kumar,[a] Magnus Willander,[b] Jai G. Sharma,[a] and Bansi D. Malhotra*,[a]

[a] Nanobioelectronics Laboratory, Department of Biotechnology, Delhi Technological University, Shahbad Daulatpur, Delhi-110042, India,

[b] Department of Science and Technology, Linköping University,SE-60174, Sweden

Abstract:

Solution processed poly (3,4-ethylenedioxythiophene):poly(styrenesulfonate) (PEDOT:PSS) - carbon nanotubes (CNT) nano-composite has been utilized for fabrication of conducting paper (CP) via dip coating. Further, high conductivity of this paper (from ~6.5×10^{-4} to 2.2×10^{-2} Scm^{-1}) obtained by treating it with formic acid (CNT/FA@CP) is due to removal of the non-conducting PSS molecules from its surface. This smart conducting platform has been used for conjugation of the anti-carcinoembronic antigen (CEA) protein for quantitative estimation of CEA, a cancer biomarker. The transmission electron microscopy (TEM), raman spectroscopy, X-ray diffraction (XRD), scanning electron microscopy (SEM), X-ray photoelectron spectroscopy (XPS), electrochemical impedance spectroscopy (EIS) and amperometric techniques have been used to characterize the low cost, flexible and environment friendly conducting BSA/anti-CEA/CNT/FA@CP) paper electrode that is found to be highly sensitive (7.8 $\mu Ang^{-1}mlcm^{-2}$) in the physiological range (2–15 $ngmL^{-1}$) of CEA. The response of the paper electrode is validated using CEA concentration of serum samples of cancer patients obtained via immunoassay technique.

Keywords: Conducting paper, PEDOT:PSS, Biosensor, Cancer

Introduction:

Corresponding author: Bansi D. Malhotra, Email: bansi.malhotra@gmail.com, Phone: +91-011-45609152, Fax: +91-011-45609310

Journal of Materials Chemistry B Accepted Manuscript

Cancer occurs due to uncontrolled growth and spread of abnormal cells and is currently a medical threat to the mankind. According to a recent report, there have been 8.2 million cancer deaths, 14.1 million new cancer cases and 32.6 million people are living with cancer (within 5 years of diagnosis) necessitating its early detection.[1-2] Carcinoembryonic antigen (CEA) is an important biomarker for the diagnosis and routine monitoring of cancer. The human CEA gene family is clustered on chromosome 19q and it comprises of 29 genes.[3] CEA (a glycoprotein) comprises of ~ 60% carbohydrate having molecular mass of ~180–200 KDa, is one of the most widely used cancer biomarker. It plays an important role in early monitoring, screening and disease recurrence. The existing techniques, including cytopathology, biopsy, enzyme linked immunosorbent assay, and visualization adjuncts can be used for detection and monitoring of cancer.[4-5] These methods are invasive, time-consuming, expensive and require highly skilled personnel. In this context, biosensors offer a simple, reliable, and user friendly detection strategy with increased assay speed, high sensitivity, low cost and require low sample volume.[6-7]

For the fabrication of biosensors, indium tin oxide, glassy carbon and gold electrodes can be used as the substrates. These electrodes have high cost, are rigid, brittle, and their fabrication requires high temperature processing and expertise , Besides this, disposability of these materials continues to be a major challenge. Therefore, there is increased demand for the development of a paper based biosensor for clinical application as these are predicted to be simple, low cost, flexible, lightweight, biocompatible, and it can be easily disposed by incineration.[8-10] Conducting paper has been found to play an important role in the ongoing transition to the development of paper based electrochemical biosensors. Coupling of paper electronic devices (such as electrodes and transistors) with biological systems provides an efficient platform for conduction of both electronic and ionic charge carriers that play a major

Journal of Materials Chemistry B Accepted Manuscript

role for communication with a desired biolmolecule.[11-14] Many methods including inkjet printing, screen printing, spin coating to modify paper substrate can be utilized for making a paper conducting. Manekkathodi *et al.* deposited thin film of ZnO by spin coating on paper and used it for fabrication of the flexible diode and UV photodetectors.[15] Määttänen *et al.* utilized inkjet printing method for fabrication of gold electrode over paper substrate. Further poly (3,4-ethylenedioxythiophene) (PEDOT) layer was electropolymerized over gold coated paper electrode for glucose detection.[16] Kumar *et al.* reported a screen printing method for producing graphite and silver ink pattern on the paper substrate. These authors electrochemically deposited polyaniline over screen printed paper electrode for cancer biomarker (sIL2Rα) detection.[17] Ge *et al.* used carbon nanotube and gultarldehyde modified paper to fabricate the electrode array of Ag/AgCl reference and carbon counter electrodes for cancer biomarker detection.[18] Su *et al.* reported gold nanoparticle modified paper device for aptamer based detection of cancer cell and *in-situ* anticancer drug screening.[19] These techniques require skilled personal, costly conducting ink (gold, silver and graphite) paste and equipments, and are time-consuming .

Conducting polymers (CPs) are a promising candidate for fabricating conducting paper due to their low cost, mechanical flexibility and solution processability.[20] The poly(3,4-ethylenedioxythiophene: poly(4-styrenesulfonate) (PEDOT:PSS) has emerged as an interesting conducting material due to its film forming ability, thermal stability and homogenous adsorption on a paper by simple dip coating method.[21-22] PEDOT:PSS consists of hydrophobic and conducting PEDOT-rich grains encapsulated by hydrophilic and insulating PSS-rich shells. The conductivity of the PEDOT:PSS can be tuned by chemical modification that depends on nature and the degree of doping.[23-26] There is a great deal of scope to improve the performance of a conducting paper sensor by integrating it with nanomaterials. In this context, carbon nanotubes

Journal of Materials Chemistry B Accepted Manuscript

have aroused much interest for application to electrochemical biosensor. This is due to their excellent electrochemical properties, large surface area, ballistic electron transport and high mechanical strength.[27-28] In addition to enhanced electrochemical reactivity, CNT-modified electrodes can be utilized to immobilize biomolecules and to minimize surface fouling.[29] These properties make CNT widely attractive for fabrication of electrochemical biosensors.

We report a facile method to obtain enhanced conductivity of PEDOT:PSS coated paper on treatment with formic acid. Doping of CNTs into the solution processed conducting paper results in improved electrochemical characteristics of the paper electrode. This low cost, flexible and environment friendly CNTs modified conducting paper has been utilized for the detection of a cancer biomarker (carcinoembryonic antigen, CEA).

2. Materials and Methods

(I) Chemicals and reagents

PEDOT:PSS (1.3 wt%, PEDOT content: 0.5wt %, PSS content: 0.8 wt%), carcinoembryonic antibody monoclonal (anti-CEA), carcinoembryonic antigen(CEA), 1-ethyl-(dimethylaminopropyl)carbodiimide hydrochloride (EDC), N-hydroxysuccinimide (NHS) and bovine serum albumin (BSA) were procured from Sigma Aldrich, India. All other chemicals like ethylene glycol, formic acid were of analytical grade and procured from Theromo Fisher Scientific, India. The deionized water obtained from Millipore water purification system was used for preparation of buffers and solution. The Whatman Filter paper #1 (GE healthcare, UK) was used as a substrate for adsorption of PEDOT:PSS with a thickness of 0.18 mm. The carboxy functionalized CNTs were a gift and used without purification.

Journal of Materials Chemistry B Accepted Manuscript

(II) Fabrication of PEDOT:PSS based conducting paper: The PEDOT:PSS aqueous solution doped with 5% EG was used to fabricate the conducting paper. The Whatman Paper #1 (1cm×3 cm) was dipped in aqueous suspension of PEDOT:PSS (1.3wt%, 5% ethylene glycol) for 1 h and was then dried at 100°C in a hot air oven,was termed as conducting paper(CP) after which it was further treated with formic acid by dipping it in formic acid for 20 min. The formic acid (FA) treated conducting paper (FA@CP) was finally dried at 100°C for about 1 h.

(III) Fabrication of CNT doped conducting paper (CNT/FA@CP): Firstly, 5 mg CNT doped into 10 ml of PEDOT:PSS aqueous solution (1.3wt%, 5% EG). Next, PEDOT:PSS/CNT composite (1.3wt%, 5% EG, 0.05wt% CNT) ultrasonicated for 1 h. It was found that CNT got highly dispersed without sedimentation in PEDOT:PSS solution. Further, Whatman paper #1 was dipped in PEDOT:PSS/CNT composite for 1 h and was then dried at 100°C in a hot air oven after which it was further treated with formic acid by dipping it in the formic acid for 20 min. The formic acid treated conducting paper was finally dried at 100°C for about 1 h. A Schematic of the experiment is demonstrated in Scheme 1.

(IV) Fabrication of paper sensor (anti-CEA/CNT/FA@CP): Anti-CEA monoclonal (20 µL, 100µg/mL) antibodies were immobilized over the CNT doped conducting paper treated with formic acid electrode (CNT/FA@CP) via formation of a covalent bond between the carboxylic group of CNT and the NH_2-terminal of the antibody via EDC-NHS coupling reaction. The anti-CEA are physically adsorbed over CNT/FA@CP electrode via electrostatic interactions between biomolecules and conducting paper. The electrode was then rinsed with phosphate buffer (PBS, 50 mM, pH 7.2, 0.9% NaCl) to remove any unbound antibodies. 0.1% of bovine serum albumin (BSA) in PBS was added to the antibody-modified electrode to block unspecific sites. After

Journal of Materials Chemistry B Accepted Manuscript

rinsing again with PBS, the electrodes were stored at 4 °C before carrying out the sensing studies.

(V) Characterization: The CNT/PEDOT:PSS nanocomposite was characterized using transmission electron microscopy (Tecnai G2 30, Ultratwin microscope), Raman spectroscopy (Varian 7000 FT-Raman) and X-ray diffraction spectroscopy (Bruker D-8 Advance, Cu Kα, λ = 1.5406 Å). The surface morphology was investigated by scanning electron microscopy (Nova Nano Sem450 and Carl Zeiss, EVO15). The conductivity of the conducting paper was measured using the four points probe technique with a low current source (LCS-02), digital microvoltmeter (DMV-001) and PID controlled oven (PID-200), SES Instruments, India. The effect of solvent on PEDOT:PSS structure was investigated by X-ray photoelectron spectroscopy (XPS) (Scienta ESCA 200). The electrochemical studies were carried out by an Autolab Potentiostat/Galvanostat (Metrohm, Netherlands) using a conventional three-electrode cell with the paper electrode as a working electrode, platinum wire as auxiliary electrode and Ag/AgCl as the reference electrode in phosphate buffer saline (PBS, 50 mM, pH 7.4) containing 5 mM $[Fe(CN)_6]^{3-/4-}$.

Journal of Materials Chemistry B Accepted Manuscript

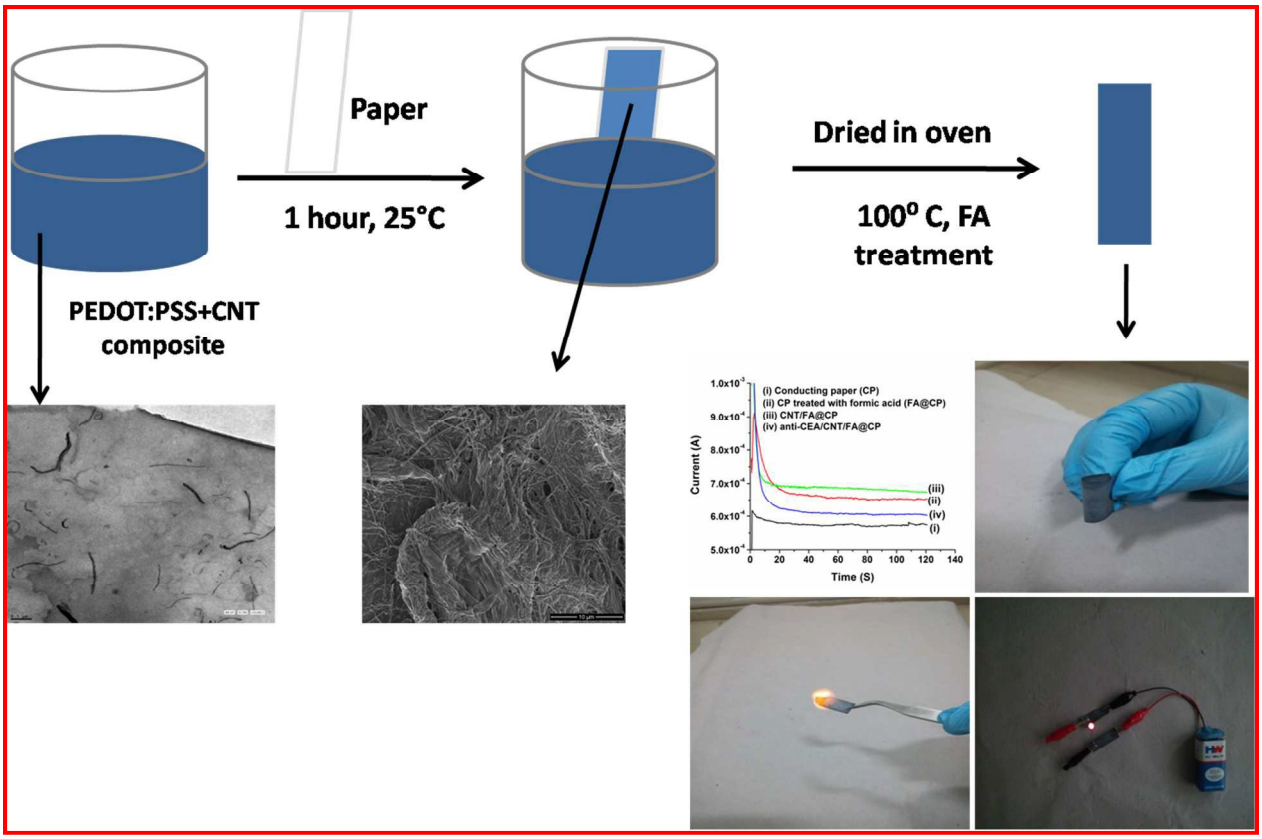

Scheme 1: Fabrication and characterization of CNT/FA@CP modified paper electrode.

Journal of Materials Chemistry B Accepted Manuscript

3. Results and discussion

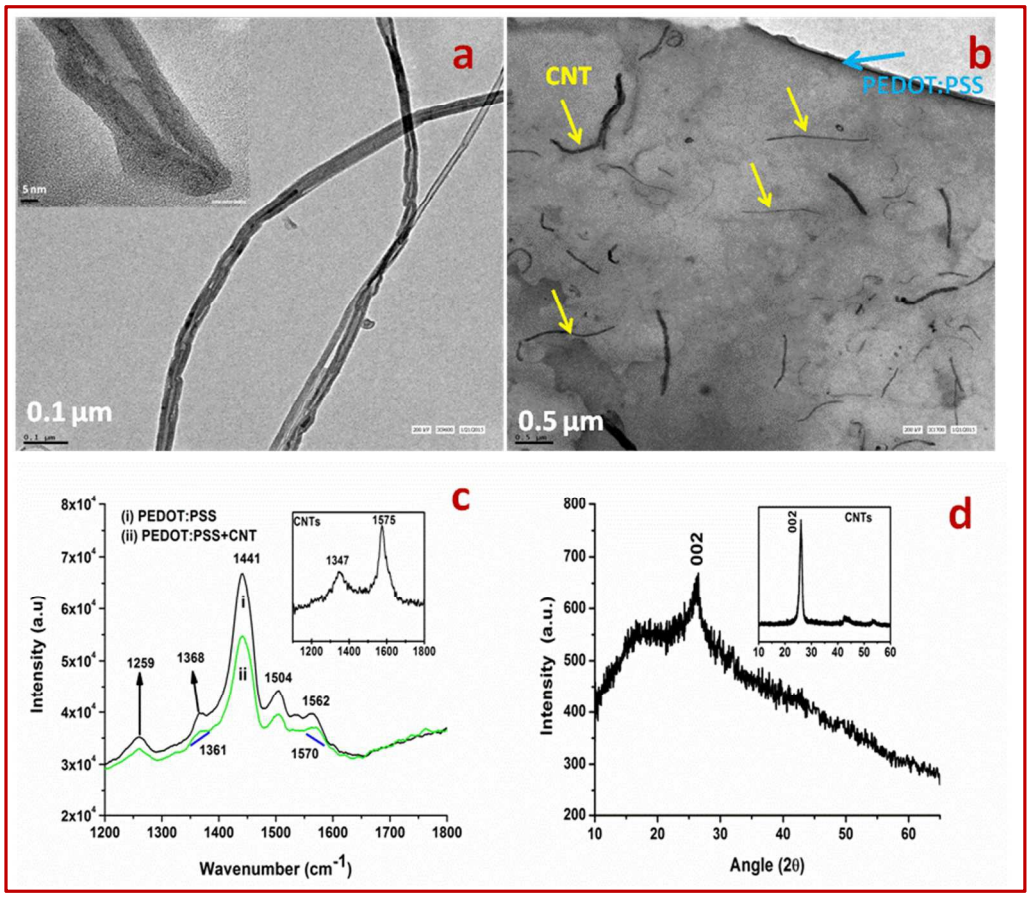

Figure 1: TEM image of (a) carbon nanotube (b) CNT/PEDOT:PSS composite (c) Raman spectrum of (i) PEDOT:PSS and (ii) PEDOT:PSS/CNT composite [Inset shows the Raman of CNTs] (d) XRD pattern of PEDOT:PSS/CNT composite and inset showing XRD of CNTs.

Figure 1a shows TEM image of the CNT that indicating linear and a tubular structure with a few microns in length. The tubular structure with diameter ranging from ~25-30 nm can be seen in the inset of Figure 1a. It appears that CNT are uniformly dispersed in PSS via non-covalent stabilization. Hydrophobic portion of polymeric chains appear to cover the carbon nanotube surface via edge-to-face aromatic interactions where as the hydrophilic part interacts with water molecules to make homogeneous dispersion of CNTs.[30] TEM image of PEDOT:PSS-CNT

Journal of Materials Chemistry B Accepted Manuscript

nanocomposite is shown in Figure 1b wherein uniformly dispersed CNT are clearly visible at the PEDOT:PSS surface. The Raman peaks seen at 1259 cm^{-1},1368 cm^{-1}, and 1441 cm^{-1} are associated with C-C in-plane symmetric stretching, C-C stretching deformation and C_α=C_β symmetric stretching vibration respectively. The C_α=C_β asymmetric stretching vibration gives rise to bands at 1504 and 1562 cm^{-1}, corresponding to thiophene rings in the middle and at the end of the chains (figure 1c).[31-32] Inset of figure 1c shows characteristic peak of CNTs at 1347 cm^{-1}due to D band and 1575 cm^{-1} attributed to G band.[29] The Raman spectrum of the PEDOT:PSS/CNT hybrid shows peak shift from 1368 to 1361 cm^{-1} and 1562 to 1570 cm^{-1} indicating existence of interactions between the CNTs and the conjugated thiophene ring of PEDOT:PSS, that can be associated with electronic density transfer between constituent.[31-32] Similarly XRD spectra also shows a sharp peak centered on 2θ value 26.2° corresponding to the (002) plane of CNTs (inset of Figure 1d shows XRD of CNTs) confirming the presence of CNTs in PEDOT:PSS amorphous polymer.[33]

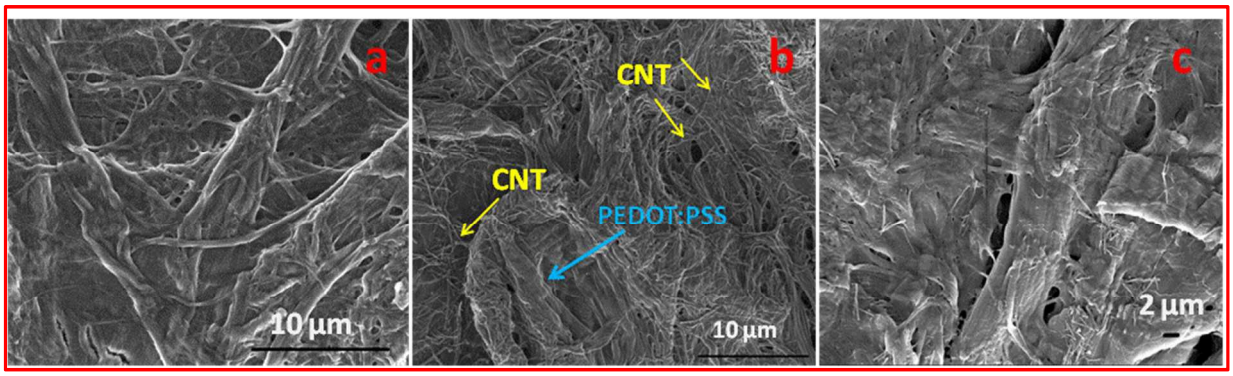

Figure 2: SEM image of (a) PEDOT:PSS coated paper (b) CNT/PEDOT:PSS coated paper (c) anti-CEA/CNT/PEDOT:PSS paper sensor

The surface morphology of the various modified electrode was investigated using scanning electron microscopy (SEM) (Figure 2). Image a shows SEM of the PEDOT:PSS coated

Journal of Materials Chemistry B Accepted Manuscript

paper, wherein conducting polymer is found to be uniformly adsorbed over the cellulose fibers of the paper. However, morphology of the PEDOT:PSS-CNT coated paper (Image b) suggests that CNT are incorporated throughout the surface. Most CNT are entangled with PEDOT:PSS and cellulose fibers while some of these are clearly visible on the surface of the polymer coated paper. SEM image of CNT/PEDOT:PSS onto ITO glass substrate confirms the presence of CNT in PEDOT:PSS film (Figure S1 in Supporting Information). However, after the antibody functionalization (image c), surface morphology of the PEDOT:PSS-CNT coated paper electrode exhibits a shiny appearance due to accumulation of the static charge, indicating successful immobilization of the antibodies. It appears that the antibody molecules cover the pores of the PEDOT:PSS-CNT coated paper surface.

The PEDOT:PSS coated paper shows electrical conductivity of 6.5×10^{-4} Scm^{-1} whereas after doping with 5% ethylene glycol, the conductivity increases to 2.1×10^{-3} Scm^{-1}. This is attributed to decreased columbic interactions between the positively charged PEDOT molecules and the negatively charged PSS that facilitate reorientation of the polymer chains resulting in enhanced charge carrier mobility. The increased crystal ordering and crystal size on addition of EG results in improved carrier mobility and electrical conductivity.[25, 34] On treatment of this paper with formic acid, EG doped conducting paper electrode shows the highest electrical conductivity value (2.4×10^{-2} S cm^{-1}) by 2 orders of magnitude compared to other solvent (methanol and sulphuric acid). The electrical conductivity enhancement is known to strongly depend on the dielectric constant of the chemicals used for treatment.[24, 26] The high dielectric constant of formic acid (58.5) screens the columbic interaction between positively charged conducting PEDOT and the negatively charged non- conducting PSS resulting in phase separation between them leading to removal of the PSSH and formation of interconnected

Journal of Materials Chemistry B Accepted Manuscript

PEDOT chains and enhanced conductivity. Further, we incorporated CNT in the PEDOT:PSS solution (1.3wt%, 5% EG, 0.05wt% CNT) for electrochemical studies since CNT are known to exhibit excellent electrochemical activity, fast electron transfer and large surface area.[27-28] Formic acid treated CNT doped conducting paper (CNT/FA@CP) retains almost similar order of conductivity value (2.2×10^{-2} Scm^{-1}) as compared to that of the formic acid treated conducting paper (FA@CP).

The optical image of the CNT modified conducting paper treated with formic acid (CNT/ FA@CP) shows high flexibility and conductivity as demonstrated in video 1 and figure 3a-d. Its simple fabrication does not require any additional steps and it can be cut into desired shape and size. This platform holds great potential for application in the paper based electrochemical devices. In figure 3c-d we demonstrate an efficient conductivity of paper electrode by lighting an LED when current is passed through multiple times folded conducting paper (video 1). It may be noted that this low-cost conducting platform can be easily decomposed by simple burning/incineration (Image 3e-f) .This is an additional advantage for electronic and biomedical waste management.

Journal of Materials Chemistry B Accepted Manuscript

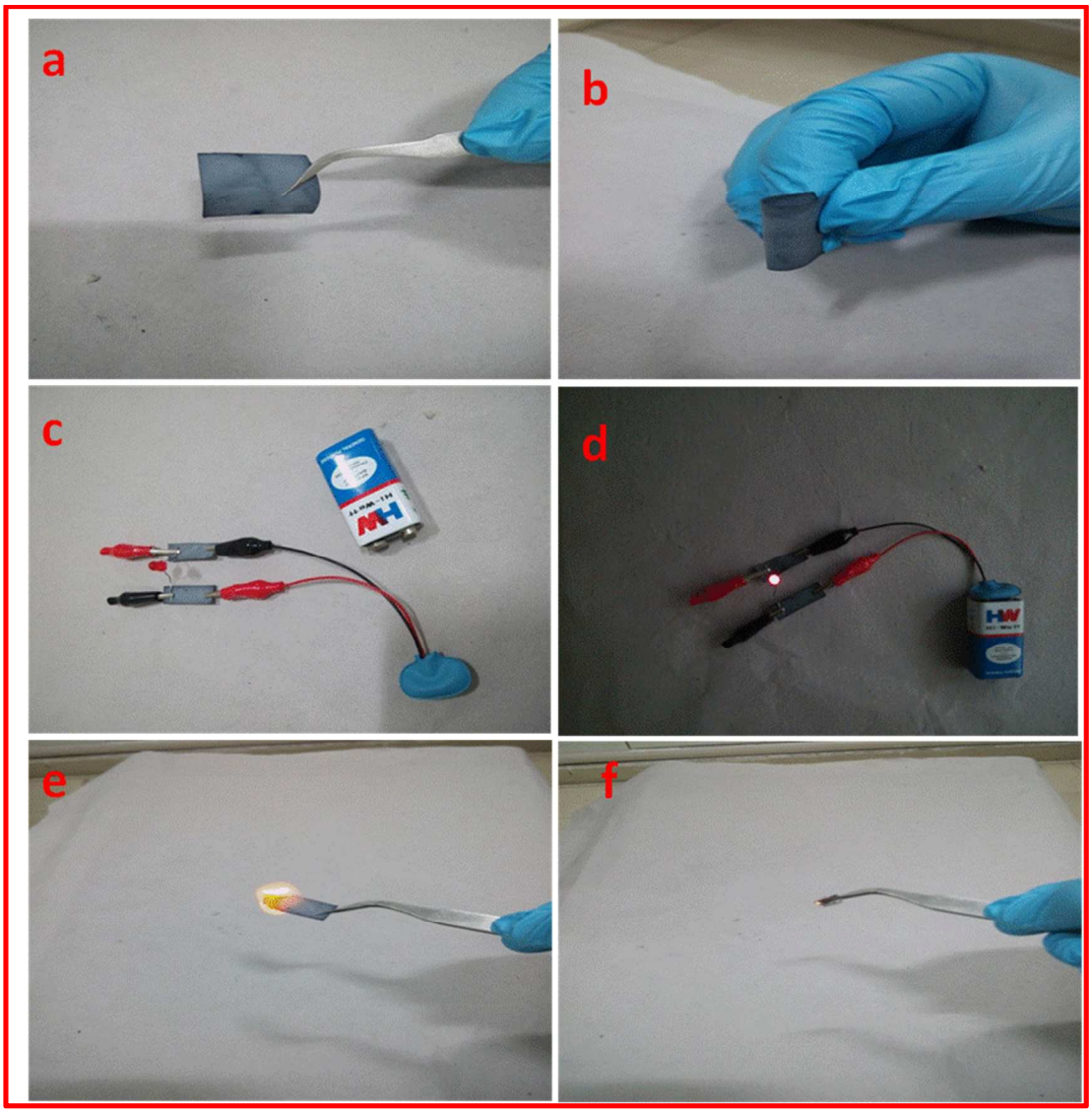

Figure 3: (a) Optical image of conductive and electrochemicaly active paper (CNT/ FA@CP) showing (b) high flexibility (c-d) Lighting an LED lamp (e-f) easy to dispose off.

Journal of Materials Chemistry B Accepted Manuscript

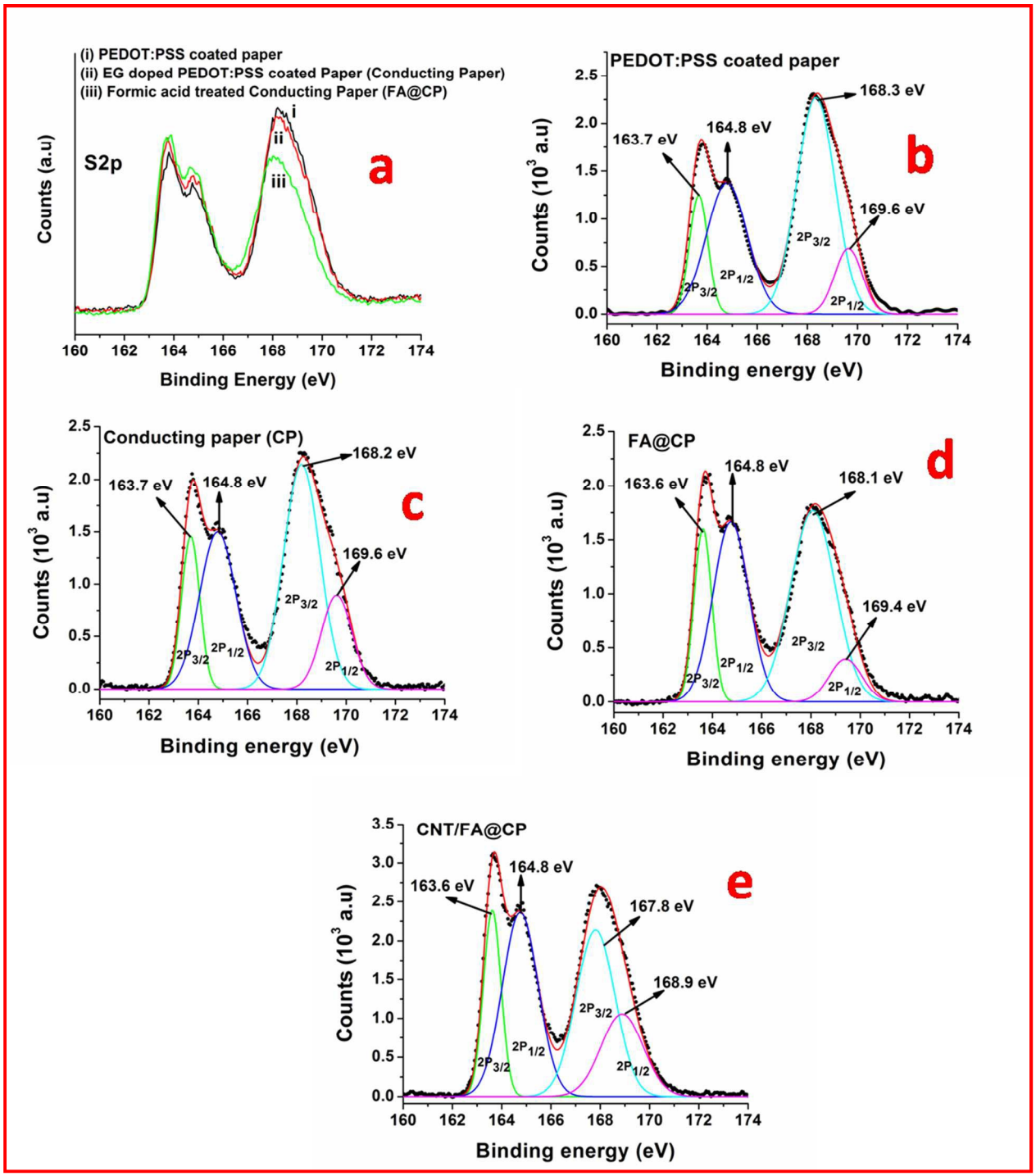

Figure 4: S (2p) XPS spectra of (a) modified papers, XPS curve fitting of (b) PEDOT:PSS coated Paper (c) Ethylene glycol doped PEDOT: PSS coated over paper i.e conducting paper (d) conducting paper treated with formic acid (FA@CP) (e) CNT doped conducting paper treated with formic acid.

Journal of Materials Chemistry B Accepted Manuscript

In PEDOT:PSS, both PEDOT and PSS contain one sulfur atom per monomer. In PSS, sulfur is present as sulfonate moiety whereas PEDOT contains sulfur in thiopene ring and thus provides different chemical environments since S(2p) electrons of PEDOT and PSS have different binding energies.[35] The S 2p band of PEDOT is found at lower binding energy whereas S 2p band of PSS is observed at higher binding energy. Each band splits into doublet of S $2p_{3/2}$ and S $2p_{1/2}$ component due to spin-orbital splitting of sulfur atom. Figure 4a shows XPS spectra of the pristine PEDOT:PSS coated paper (curve i), EG doped PEDOT:PSS paper (conducting paper) (curve ii), formic acid treated conducting paper (curve iii). The observed slight change in peak intensity of conducting paper as compared to that of the PEDOT:PSS coated paper may be assigned to the conformational changes in PEDOT:PSS polymer. However after formic acid treatment there is decrease in peak intensity of PSS indicating exfoliation of PSS from conducting paper surface. Figure 4b shows XPS spectra of the pristine PEDOT:PSS coated paper that has been deconvoluted into the characteristic binding energy peaks. The S $2p_{3/2}$(S $2p_{1/2}$) peak at the binding energy near 163.7 (164.8) eV corresponds to sulfur atom of the PEDOT and the S $2p_{3/2}$ (S $2p_{1/2}$) peak seen at the binding energy near 168.3 (169.6) eV is due to sulfur atom present in PSS.[36-37] The binding energy positions of these bands are almost same as in the case of the conducting paper (figure 4c). However, after the formic acid treatment, S 2p peak of PSS is shifted to lower energy level (Figure 4d). It is observed that PSS peak of CNT/FA@CP (Figure 4e) is shifted towards the lower binding energy as compared to that of FA@CP around -0.3. The presence of (-0.5) eV is due to high electron density in PSS because of charge transfer from CNT to electronegative sulfur atom indicating existence of interactions between the CNT and the conjugated thiophene ring of PEDOT:PSS.[33]

Journal of Materials Chemistry B Accepted Manuscript

In PEDOT:PSS, PEDOT molecules are conductive in nature and are surrounded by the non-conductive PSS molecules.[21] On being treated with formic acid, this core-shell structure of the PEDOT:PSS in conducting paper changes from coiled to partially linear due to ejection of PSS molecules that are perhaps responsible for enhanced connectivity between PEDOT chains. Therefore energy barrier for charge hopping is lowered resulting in enhanced charge transfer among the PEDOT chains. The ratio of PEDOT to PSS can be estimated from area under the curve. It is found that, there is no significant change in PEDOT to PSS ratio between PEDOT:PSS coated paper (1/1.33) and conducting paper (1/1.30). However, the ratio of PEDOT to PSS increases from 1/1.30 to 1/1.04 after conducting paper is treated with formic acid confirming removal of ~20% PSS from the surface. It appears that exclusion of PSS due to formic acid treatment is perhaps responsible for better connectivity between PEDOT chain that in turn result in increased conductivity.

Figure 5a shows results of the chronoamperometric studies obtained for (i) conducting paper, [CP] (ii) conducting paper treated with formic acid, [FA@CP] (iii) CNT doped conducting paper treated with formic acid, [CNT/FA@CP] (iv) anti-CEA immobilized over CNT/FA@CP, [anti-CEA/CNT/FA@CP] at 2V on every 0.1 s. The increased electrochemical response current of the FA@CP electrode (~0.65mA) than that of the CP electrode (~0.57mA) is attributed to increased conductivity of the electrode due to removal of PSS from the film surface. Further increase in the electrochemical current value of CNT/FA@CP electrode (~0.68mA) can be assigned to high electrochemical activity of CNT that enhances permeability of the redox couple $[Fe(CN)_6]^{3-/4-}$. Next, decrease in the value of electrochemical current observed after immobilization of anti-CEA onto CNT/FA@CP electrode (~0.60mA) is attributed to the

Journal of Materials Chemistry B Accepted Manuscript

hindrance caused by the CEA antibodies to the electron transport indicating immobilization of anti-CEA.

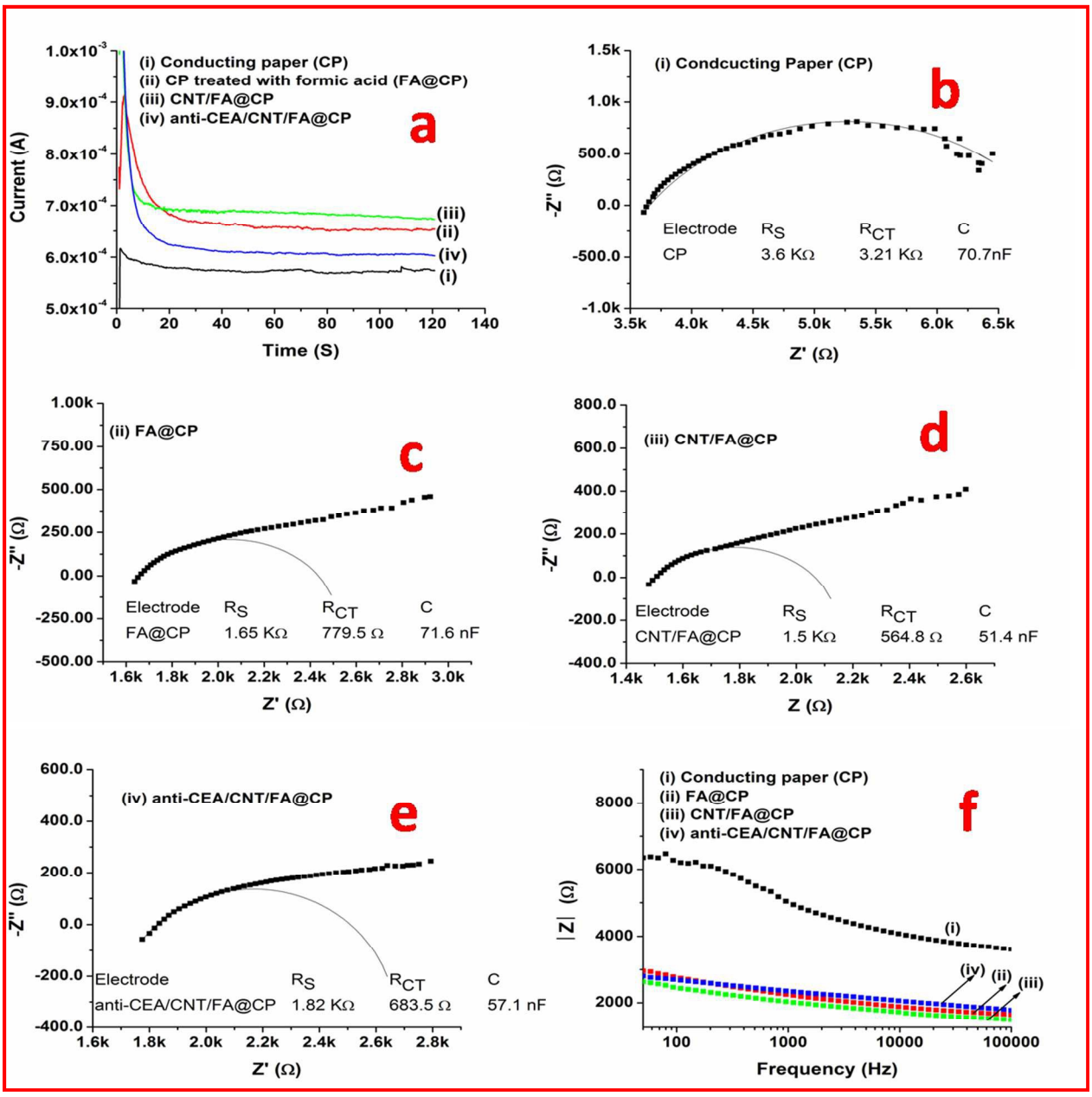

Figure 5: Electrochemical characterization of modified paper electrode (a) chronoamperometric studies of modified paper electrode. Impedance spectra of (b) conducting paper (c) conducting paper treated with formic acid (FA@CP) (d) CNT modified conducting paper treated with formic acid (CNT/FA@CP) (e) anti-CEA/CNT/FA@CP paper electrode and circuit were fitted with equivalent randles circuit $R_S(R_{CT}C)$. (f) Bode plot of different modified electrode.

Journal of Materials Chemistry B Accepted Manuscript

Electrochemical impedance spectroscopy (EIS) is an effective tool for investigating interfacial properties of the surface modified electrodes. Figure 5 shows the Nyquist plot obtained for (b) conducting paper, [CP] (c) conducting paper treated with formic acid, [FA@CP] (d) CNT doped FA@CP, [CNT/FA@CP] and (e) anti-CEA immobilized over CNT/FA@CP, [anti-CEA/CNT/FA@CP] in PBS solution containing 5 mM $[Fe(CN)6]^{3-/4-}$ at 0.03V (biasing potential) in the frequency range, 100KHz to 50 Hz. The diameter of the semicircle in the Nyquist plot yields magnitude of the charge transfer resistance (R_{ct}) of electrode that depends on the dielectric features of the electrode/electrolyte interface. It can be seen that R_{CT} value of the conducting paper electrode (3.2 KΩ, figure 5b) decreases after the formic acid treatment (779.5 Ω, figure 5c). This is assigned to the high dielectric constant of the formic acid that facilitates decreased coulombic interaction between PEDOT and PSS leading to removal of the PSS molecule. The exclusion of PSS (negatively charged and non-conducting in nature) from the conducting paper provides increased exposure of the inter-connected PEDOT chains (positively charged and conducting in nature) that promotes permeability of redox probe, $[Fe(CN)6]^{3-/4-}$ to the surface of FA@CP electrode. The value of R_{CT} (564.8 Ω, Figure 5d) for the CNT/FA@CP electrode is smaller than that of the FA@CP electrode (779.5 Ω). This may be attributed to excellent electrochemical properties and larger surface area of CNT that are incorporated in the PEDOT:PSS matrix resulting in increased permeability of the $[Fe(CN)_6]^{3-/4-}$ to the surface of CNT/FA@CP paper electrode. Further, increase in the value of R_{CT} (683.5 Ω, Figure 5e) of anti-CEA/CNT/FA@CP is attributed to the hindrance caused by the macromolecular structure of the antibodies that perhaps obstruct electron transfer owing to their insulating nature. These results also confirm functionalization of the CNT/FA@CP electrode with anti-CEA. The heterogeneous

Journal of Materials Chemistry B Accepted Manuscript

electron transfer rate constant (K_{ct}) of CNT/FA@CP and FA@CP electrode can be calculated using equation 1.[38]

$$K_{ct} = \frac{\mathrm{RT}}{n^2F^2AR_{ct}[S]} \ldots\ldots\ldots\ldots\ldots\ldots (1)$$

where R is the gas constant, T is absolute temperature, F is the Faraday constant, A is the electrode area (cm^2), [S] is the concentration of redox probe (mol/cm^3) and n is the number of transferred electrons per molecule of the redox probe. The heterogeneous electron transfer rate constant (K_{ct}) value of the CP, FA@CP and CNT/FA@CP has been found to be 1.66×10^{-7} cm s^{-1}, 6.83×10^{-5} cm s^{-1} and 9.43×10^{-5} cm s^{-1}, respectively. This indicates that the CNT/FA@CP electrode exhibits faster electron transfer kinetics as compared to that of the other modified paper electrodes. Thus incorporation of CNT results in improved electrochemical activity of the paper electrode (CNT/FA@CP). Interestingly, K_{ct} of CNT/FA@CP electrode is found to be nearly 5 times higher compared to our previous work where in PEDOT:PSS-RGO composite was used to fabricate conducting paper using ethylene glycol.[39]

The solution resistance (R_s) is found to be the highest (3.6 KΩ) for CP electrode as compared to that of the other modified electrodes FA@CP (1.6 KΩ), CNT/FA@CP (1.5 KΩ) and anti-CEA/CNT/FA@CP (1.8 KΩ). R_S depends on the type of ions, ionic concentration, temperature and the electrode surface.[40] This suggests that after the formic acid treatment, morphology of CP electrode changes due to the removal of PSS leading to lower Rs value. Figure 5f shows the Bode plot representing the impedance modulus (|Z|) vs. frequency for the modified paper electrodes. The FA@CP, CNT/FA@CP and anti-CEA/CNT/FA@CP electrodes exhibit low |Z| compared to CP in the frequency range, 50 Hz to 100 KHz, confirming increased electrochemical activity due to removal of non conducting PSS molecule. The values of

Journal of Materials Chemistry B Accepted Manuscript

electrical conductivity and electrochemical properties of modified paper electrodes are summarized in Table 1.

Table 1: Conductivity and electrochemical properties of modified paper electrode.

S.No.	Material coated on Paper	Conductivity	Charge transfer resistance (R_{CT})	Solution Resistance (R_S)	Heterogeneous electron transfer rate constant (K_{ct})
1.	PEDOT:PSS+ EG (CP)	2.1×10^{-3} Scm^{-1}	3.21 KΩ	3.6 KΩ	1.66×10^{-7} cm s^{-1}
2.	PEDOT:PSS+ EG treated with Formic acid (FA@CP)	2.4×10^{-2} Scm^{-1}	779.5 Ω	1.65 KΩ	6.83×10^{-5} cm s^{-1}
3.	PEDOT:PSS+ EG + CNT treated with Formic acid (CNT/ FA@CP)	2.2×10^{-2} Scm^{-1}	564.8Ω	1.5 KΩ	9.43×10^{-5} cm s^{-1}

The electrochemical response studies (Figure 6a) have been conducted by varying the concentration of carcinoembryonic antigen (CEA) from 1 to 100 ng/ml in PBS (50mM, pH 7.4, 0.9% NaCl) containing 5 mM $[Fe(CN)_6]^{3-/4-}$ using chronoamperometry with an incubation time of 15 min. The magnitude of current decreases on addition of CEA due to formation of electrically insulating antigen–antibody complexes produced due to specific interaction of the CEA and anti-CEA that may block the electron transfer via redox probe, $[Fe(CN)_6]^{3-/4}$ at the paper electrode surface. Figure 6(b) shows the calibration curve obtained between response current and CEA concentration (curve i). It is found that the amperometric current decreases upto 25 ng/mL after which it increases and reaches saturation upto 100 ng/ml. However, a linear relationship obtained between 2-15 ng/mL with a sensitivity of 7.7 μAng^{-1}mLcm^{-2} and follows Equation (2)

Journal of Materials Chemistry B Accepted Manuscript

$$I(A) = -7.8\ \mu A\ mL\ ng^{-1} \times [CEA\ concentration] + 528\ \mu A;\ R^2 = 0.95$$

A control experiment was performed to check cross reactivity of the paper sensor with CEA antigen in the absence of antibodies (curve ii). However, no significant change in current response was observed for the BSA/CNT/FA@CP in the absence of antibodies as a function of CEA concentration. The repeatability of bioelectrode was confirmed by repeating each experiment 3 times and the error bars are included based on RSD value.

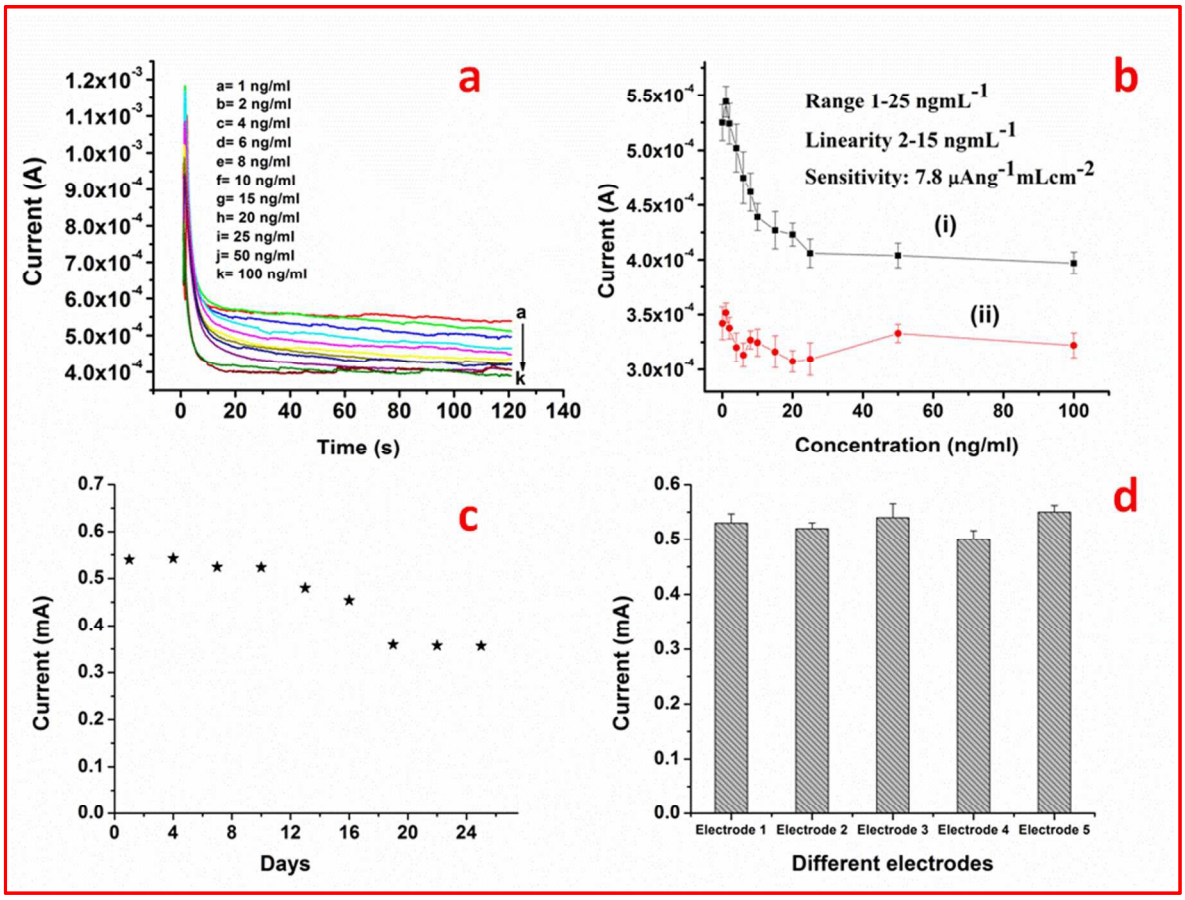

Figure 6: (a) Electrochemical response studies of the BSA/anti-CEA/CNT/FA@CP paper electrode obtained as a function of CEA concentration (1-100 $ngmL^{-1}$) using chronoamperometry and (b) calibration plot between the magnitudes of current recorded and CEA concentration (curve i); control experiment in absence of antibody (curve ii). (c) Current response time of BSA/anti-CEA/CNT/FA@CP paper electrode as a function of time (day) (d) Current response

Journal of Materials Chemistry B Accepted Manuscript

time of five different BSA/anti-CEA/CNT/FA@CP paper electrodes fabricated using the same set of procedure in presence of CEA concentration ($2ngmL^{-1}$).

CEA is traditionally, determined by gold standard technique for proteinseous molecules i.e ELISA to diagnose and monitor cancer. This method usually involves a complex procedure, is time-consuming and is expensive. It is thus desirable to develop techniques that are low cost, easy to use, are rapid, sensitive and do not require any laboratory infrastructure for the CEA estimation. Therefore attempts have been made to estimate CEA concentration in serum by using BSA/anti-CEA/CNT/FA@CP bioelectrode to evaluate the feasibility of the proposed paper sensor. The blood samples were collected from patient and processed at Rajiv Gandhi Cancer Institute & Research Centre (RGCI&RC) in Rohini, Delhi, India after the ethical approval by the Institutional Review board (Nos. RGCIRC/IRB/61/2014). We also obtained ethical approval of Institutional Ethical and Biosafety Committee, DTU (R.NO.:BT/IEBC/2014/714). The concentration of CEA in serum of cancer patients was measured at RGCI&RC using the VITROS CEA Reagent Pack and the VITROS CEA Calibrators on the VITROS ECi/ECiQ Immunodiagnostic Systems, the VITROS 3600 Immunodiagnostic System and the VITROS 5600 Integrated System using Intellicheck® Technology. An immunometric immunoassay technique was used. It can be seen that a reasonable correlation exists between (a) CEA concentration in serum samples determined by immunometric immunoassay technique and (b) standard concentration of CEA (Table 2). The results exhibit reasonable relative standard deviation (%RSD) indicating high accuracy of paper sensor.

Journal of Materials Chemistry B Accepted Manuscript

S. No.	CEA concentration ($ngmL^{-1}$) Determined using ELISA	Amperometric current (mA) obtained with Standard CEA sample	Amperometric current (mA) obtained with serum sample	%RSD
1	2.37	0.518	0.517	0.2
2	4.03	0.501	0.507	0.8
3	5.57	0.485	0.487	0.3
4	5.96	0.474	0.493	2.81
5	10	0.439	0.482	6.5

Table 2: Determination of carcinoembryonic antigen concentration in serum samples using BSA/anti-CEA/CNT/ FA@CP paper electrode

The storage stability of this paper sensor was monitored at an interval of 3 days as shown in figure 6c. It was found that the paper immunoelectrode (BSA/anti-CEA/CNT/FA@CP) retained about 82% activity even after 18 days when stored at 4°C after which the current response decreased to less than 70% in about 25 days. This indicates that the fabricated paper immunoelectrode exhibits reasonably good stability at least for 18 days. Figure 6d indicates electrochemical response of five different paper immunoelectrodes (BSA/anti-CEA/CNT/FA@CP) fabricated under the same set of conditions in presence of CEA concentration (2 $ngmL^{-1}$). It is found that this paper immunoelectrode shows good reproducibility for five different electrodes with constant surface area as is evident by standard error of less than 5% (mean value = 528μA). Further, each measurement was repeated 3 times for each electrode and the error bars are included accordingly.

The sensing characteristics of paper sensor are summarized in Table S1 along with those reported in literature. It can be seen that sensitivity of the paper electrode is much higher than that of the other reported electrodes (gold, glassy carbon and ITO electrode) and can be used to

Journal of Materials Chemistry B Accepted Manuscript

differentiate two lower value of CEA concentration .These results show that paper based electrochemical sensor is a better candidate over conventional electrodes.

To attest the environment friendliness, these paper electrodes were decomposed by incineration. The resulting ash was investigated by energy dispersive X-ray (EDX) technique. EDX results confirm the presence of only carbon, oxygen, sodium, phosphorous and potassium; no toxic metals were detected (Figure S2 in supporting information).

4. Conclusions:

The nanocomposite of poly(3,4-ethylenedioxythiophene):poly(styrenesulfonate) (PEDOT:PSS) and carbon nanotubes (CNT) has been used to fabricate conducting paper (CNT/CP). It is found that conductivity of this paper increases by 2 orders of magnitude on being treated with formic acid (CNT/FA@CP) due to removal of the non-conducting molecule PSS from electrode surface. This paper has been utilized to fabricate nanomaterial modified conducting paper electrode for estimation of carcinoembryonic antigen (CEA). The fabricated BSA/anti-CEA/CNT/FA@CP bioelectrode exhibits high sensitivity of 7.8 $\mu A(ng/ml)^{-1}cm^2$ and a linear range of 2-15 $ngmL^{-1}$. The CEA concentration has been estimated in serum samples by using BSA/anti-CEA/CNT/FA@CP bioelectrode to evaluate the feasibility of the proposed paper electrode. This simple fabrication method provides flexible, environment friendly and cost effective platform that can be utilized for flexible electronics, microfludics, energy storage devices and point of care devices etc. And efforts should be made to improve the stability and performance of the BSA/anti-CEA/CNT/FA@CP platform for CEA detection by selection of the suitable dopant and solvent.

Journal of Materials Chemistry B Accepted Manuscript

Acknowledgements

We thank the Vice Chancellor, Delhi Technological University (DTU), Delhi, India for providing the facilities. Saurabh Kumar is thankful to DTU for the award of financial assistance and Dr Saurabh srivastava, DTU for scientific discussion during preparation of manuscript. SK is thankful to Dr. LS Meena, Institute of Genomics & Integrative Biology (IGIB) for TEM facilities and Dr Birendra K. Yadav, Dr D C Doval, Rajiv Gandhi Cancer Institute & Research Centre for providing patient samples. The authors are also thankful to Sandeep Mishra, Central Facility Lab, Delhi Technological University for EDX.

References:

1. L. Wu and X. Qu, *Chem. Soc. Rev.* 2015, 44, 2963-2997.
2. I. A. f. R. o. Cancer, *World Health Organization, www. cancerresearchuk. org*, 2012.
3. M. J. Duffy, *Clinical chemistry*, 2001, 47, 624-630.
4. I. E. Tothill, Semin cell dev biol, 2009, 20, 55-62.
5. S. Kumar, S. Kumar, S. Tiwari, S. Srivastava, M. Srivastava, B. K. Yadav, S. Kumar, T. T. Tran, A. K. Dewan and A. Mulchandani, *Adv. Sci.*, 2015, 2, 1500048.
6. B. D. Malhotra and A. Chaubey, *Sens. Actuat. B-Chem.*, 2003, 91, 117-127.
7. S. K. Arya and S. Bhansali, *Chem. Rev.*, 2011, 111, 6783-6809.
8. A. W. Martinez, S. T. Phillips, G. M. Whitesides and E. Carrilho, *Anal. chem.*, 2009, 82, 3-10.
9. E. W. Nery and L. T. Kubota, *Anal. Bioanal. chem.*, 2013, 405, 7573-7595.
10. J. Hu, S. Wang, L. Wang, F. Li, B. Pingguan-Murphy, T. J. Lu and F. Xu, *Biosens. Bioelectron.*, 2014, 54, 585-597.
11. L. Wang, W. Chen, D. Xu, B. S. Shim, Y. Zhu, F. Sun, L. Liu, C. Peng, Z. Jin and C. Xu, *Nano lett.*, 2009, 9, 4147-4152.
12. J. R. Windmiller, A. J. Bandodkar, G. Valdés-Ramírez, S. Parkhomovsky, A. G. Martinez and J. Wang, *Chem. Comm.*, 2012, 48, 6794-6796.

Journal of Materials Chemistry B Accepted Manuscript

13. N. Ruecha, R. Rangkupan, N. Rodthongkum and O. Chailapakul, *Biosens. Bioelectron.*, 2014, 52, 13-19.
14. A. C. Glavan, D. C. Christodouleas, B. Mosadegh, H. D. Yu, B. S. Smith, J. Lessing, M. T. Fernández-Abedul and G. M. Whitesides, *Anal. chem.*, 2014, 86, 11999-12007.
15. A. Manekkathodi, M. Y. Lu, C. W. Wang and L. J. Chen, *Adv. Mater.*, 2010, 22, 4059-4063.
16. A. Määttänen, U. Vanamo, P. Ihalainen, P. Pulkkinen, H. Tenhu, J. Bobacka and J. Peltonen, *Sens. Actuat B- Chem.*, 2013, 177, 153-162.
17. S. Kumar, K. K. Jagadeesan, A. G. Joshi and G. Sumana, *RSC Adv.*, 2013, 3, 11846-11853.
18. S. Ge, L. Ge, M. Yan, X. Song, J. Yu and J. Huang, *Chem. Comm.*, 2012, 48, 9397-9399.
19. M. Su, L. Ge, S. Ge, N. Li, J. Yu, M. Yan and J. Huang, *Anal. chim. Acta*, 2014, 847, 1-9.
20. V. Saxena and B. Malhotra, *Curr. Appl. Phys.*, 2003, 3, 293-305.
21. U. Lang, E. Müller, N. Naujoks and J. Dual, *Adv. Funct. Mater.*, 2009, 19, 1215-1220.
22. D. Tobjörk and R. Österbacka, *Adv. Mater.*, 2011, 23, 1935-1961.
23. J. Kim, J. Jung, D. Lee and J. Joo, *Synth. Met.*, 2002, 126, 311-316.
24. D. Alemu, H.-Y. Wei, K.-C. Ho and C.-W. Chu, *Energy & Environ. Sci.*, 2012, 5, 9662-9671.
25. Q. Wei, M. Mukaida, Y. Naitoh and T. Ishida, *Adv. Mater.*, 2013, 25, 2831-2836.
26. D. A. Mengistie, M. A. Ibrahem, P.-C. Wang and C.-W. Chu, *ACS appl. mater inter.*, 2014, 6, 2292-2299.
27. V. V. Shumyantseva, L. V. Sigolaeva, L. E. Agafonova, T. V. Bulko, D. V. Pergushov, F. H. Schacher and A. I. Archakov, *J. Mater. Chem. B*, 2015, 3, 5467-5477.
28. S. Soylemez, F. E. Kanik, S. D. Uzun, S. O. Hacioglu and L. Toppare, *J. Mater. Chem. B*, 2014, 2, 511-521.
29. C. Singh, S. Srivastava, M. A. Ali, T. K. Gupta, G. Sumana, A. Srivastava, R. Mathur and B. D. Malhotra, *Sens. Actuat. B-Chem.*, 2013, 185, 258-264.
30. S. Razdan, P. K. Patra, S. Kar, L. Ci, R. Vajtai, A. Kukovecz, Z. Kónya, I. Kiricsi and P. M. Ajayan, *Chem. Mater.*, 2009, 21, 3062-3071.
31. T. Ji, L. Tan, X. Hu, Y. Dai and Y. Chen, *Phys. Chem. Chem. Phys.*, 2015, 17, 4137-4145.

Journal of Materials Chemistry B Accepted Manuscript

32. G. Guan, Z. Yang, L. Qiu, X. Sun, Z. Zhang, J. Ren and H. Peng, *J. Mater. Chem. A*, 2013, 1, 13268-13273.
33. J. Li, J.-C. Liu and C.-J. Gao, *J. poly. Res.*, 2010, 17, 713-718.
34. J. Ouyang, C. W. Chu, F. C. Chen, Q. Xu and Y. Yang, *Adv. Funct. Mater.*, 2005, 15, 203-208.
35. X. Crispin, F. Jakobsson, A. Crispin, P. Grim, P. Andersson, A. Volodin, C. Van Haesendonck, M. Van der Auweraer, W. R. Salaneck and M. Berggren, *Chem. Mater.*, 2006, 18, 4354-4360.
36. J. P. Thomas, L. Zhao, D. McGillivray and K. T. Leung, *J. Mater. Chem. A*, 2014, 2, 2383-2389.
37. H.-S. Park, S.-J. Ko, J.-S. Park, J. Y. Kim and H.-K. Song, *Sci. Rep.*, 2013, 3.
38. A. Bardea, E. Katz and I. Willner, *Electroanalysis*, 2000, 12, 1097-1106.
39. S. Kumar, S. Kumar, S. Srivastava, B. K. Yadav, S. H. Lee, J. G. Sharma, D. C. Doval and B. D. Malhotra, *Biosens. Bioelectron.*, 2015, 73, 114-122.
40. N. Sekar and R. P. Ramasamy, *J Microb Biochem Technol .,* 2013, S6, 004.

Journal of Materials Chemistry B Accepted Manuscript